

# Robust fault-tolerant attitude tracking with guaranteed prescribed performance

Chengfei Yue<sup>1</sup>, Feng Wang<sup>1\*</sup>, Xibin Cao<sup>1</sup>, Qiang Shen<sup>2</sup>, Xueqin Chen<sup>1</sup>

*1, Research Centre of Satellite Technology, Harbin Institute of Technology,  
Harbin 150001, China*

*2, School of Aeronautics and Astronautics, Shanghai Jiao Tong University,  
Shanghai 200240, China*

---

## Abstract

The robust fault-tolerant (FT) attitude tracking control problem with guaranteed prescribed performance is addressed in this paper. We consider the actuator fault, misalignment, sensor fault and external disturbance simultaneously and incorporate the  $L_2$  control allocation (CA) method to minimize the use of faulty actuators. To guarantee the prescribed performance such as the steady-state tracking error, convergence rate, as well as overshoot and undershoot, the constrained quaternion error is transformed to an unconstrained state, whose stabilization is proven to be sufficient and necessary to guarantee the performance requirement. With the utilization of the transformed state and the compromised angular velocity error suffering from gyro faults, a novel adaptive sliding mode FT control law with CA is developed. Ultimate uniform boundedness of the compromised angular velocity error and transformed state is ensured to satisfy the specified tracking performance. Numerical simulations are conducted on a rigid spacecraft to illustrate the efficiency of the proposed robust FT control law.

*Keywords:* Prescribed performance, Fault tolerant control, Sensor fault, Control allocation, Adaptive control

---

*Email addresses:* chengfei\_yue@163.com(Chengfei Yue<sup>1</sup>), wfhitsat@hit.edu.cn  
(Feng Wang<sup>1\*</sup>), xbciao@hit.edu.cn (Xibin Cao<sup>1</sup>), qiang.shen@hotmail.com  
(Qiang Shen<sup>2</sup>), cxqhit@163.com (Xueqin Chen<sup>1</sup>)

## 1. Introduction

The tracking problem has been studied extensively and a great number of control strategies have been developed, such as the PID control [1], sliding mode control [2, 3], adaptive control [4, 5], geometric control [6], to mention a few. Through these proposed control strategies, various problems corresponding to different working scenarios, for instance, actuator fault [7], actuator misalignment [8], absence of measurement [9] and etc., have been solved. The differences among these existing works usually lie with either the presence of disturbances/actuator faults/misalignments or the availability of certain measurements related to the states or parameters of the spacecraft [10, 11]. In this paper, we consider attitude tracking control problem of a rigid spacecraft suffering from actuator faults (partially lose effectiveness or complete failure), actuator misalignments, unpredicted disturbances and imprecise angular velocity measurement due to sensor faults simultaneously. In addition, an  $L_2$  optimized control allocation (CA) is incorporated in the controller design to minimize the use of the faulty actuator, and pre-defined performance requirements of the tracking error are also considered.

To cope with the actuator fault and enhance the system reliability, various fault-tolerant (FT) methods [12] and the underactuated control strategies [13] have been proposed. The common foundation of both active and passive FT strategies is the system redundancy [14], which provides the possibility to use the CA strategy in controller design. Reynolds et al. investigated the  $L_\infty$ -CA method in [15]. Verbin et al. and Cao et al. further extended this method and designed a braking curve based on the  $L_\infty$ -CA method to govern a time efficient maneuver [16, 17]. Härkegård and Glad investigated the equivalence of the  $L_2$ -CA to an overactuated optimal control with some quadratic performance index [18]. Alwi and Edwards developed a FT control strategy incorporating with  $L_2$ -CA method when actuators suffered from partially lose effectiveness and/or complete failures [19]. Shen et al. extended Alwi's result to FT tracking control problem [20]. In this paper, we will use the CA method in [20] to handle the

FT tracking control problem when the spacecraft suffers from actuators faults, misalignments and external disturbances simultaneously.

In the aforementioned FT tracking controller design, accurate system states for feedback are required. However, the imprecision of the measurement exists due to measurement noise and/or sensor fault. The discrepancy between the measured value and actual value will become even larger when cyber attackers gain access to the sensing platforms to manipulate system measurement data [21]. Therefore, taking the measurement error into consideration in controller design is of paramount importance. Mercker and Akella solved the attitude tracking problem with vector measurements and unknown gyro bias by reparameterizing the gyro-bias parameters [10]. Benallegue et al. overcame the certainty-equivalence principle with separate observer/controller design in [10] and developed an adaptive control strategy to handle the gyro bias [22]. Peng et al. even investigated the control problem with unknown control directions[23]. In this paper, the measurement error is assumed to be a state-related bounded time-varying function. The compromised measurement corrupted by the measurement error are used in feedback to develop the tracking controller and the proposed control strategy accommodate the sensor error automatically.

Another practically important consideration in developing controller is to guarantee the predefined or prescribed transient performance. Bechlioulis and Rovithakis stated that the prescribed performance means “tracking error converges to a predefined arbitrarily small residual set, with convergence rate no less than a prespecified value, exhibiting maximum overshoot as well as undershoot less than some sufficiently small preassigned constant value”, and they also developed adaptive control strategy with prescribed performance for strict feedback system and multi-output affine system respectively in [24] and [25]. Song et al. extended the guaranteed transient control method to FT tracking control system [26]. The result in spacecraft attitude tracking with prescribed performance is rare. Hu et al. considered this problem with actuator fault and proved the stability via Lyapunov method [27], but the actuator misalignment and CA strategy are not considered. Luo et al. also developed tracking con-

troller for spacecraft system with prescribed performance in [28, 29]. However, the attitude is parameterized by modified rodriques parameters (MRP), which is not practically used in developing attitude controller.

In this paper, we concentrate on developing a quaternion-based robust prescribed performance guaranteed controller incorporating CA method for the spacecraft system suffering from actuator fault, misalignment, external disturbances and imprecise angular velocity measurement due to noise or sensor fault simultaneously. First, the prescribed transient and desired behavioral bounds of the tracking error is transformed into an equivalent unconstrained state. The constraints of the transformed state correspond to the prescribed performance boundary and thus the boundedness of these transformed states is sufficient and necessary to guarantee the prescribed performance. Then a sliding mode surface with the utilization of these states are constructed, and an adaptive sliding mode FT control strategy is proposed to stabilize the sliding vector, the transformed states and estimation error. Comparing with the existing literature [20, 24, 29], and etc. , contributions can be summarized as:

- The CA technique is incorporated in robust FT attitude tracking controller design to accommodate the actuator fault, misalignment, fault estimation error and external disturbances simultaneously. The benefit of incorporating CA logic is that faulty actuators are minimally used or even isolated when the actuator fails completely, which prevents further damages to actuators and spacecraft attitude control system.
- The compromised angular velocity due to imprecision in the angular velocity measurement is utilized as feedback for attitude tracking controller design. This enhances the system reliability against sensor error or velocity measurement inaccuracy, and enables the employment of low-cost sensors to measure the angular velocity.
- The prescribed performance, i.e. steady-state error, converge rate, overshoot as well as undershoot, is guaranteed by the proposed control strategy, which is not considered in [20]. Consequently, the efficiency of the

spacecraft may be improved with the guaranteed performance and potential damages to the spacecraft caused by poor tracking performance are avoided. In addition, since the vector part of the quaternion is forced to gradually converge according to the prescribed performance, the common unwinding phenomenon in continues quaternion feedback control is also avoided.

The remaining part of this paper is organized as follows. Section II formulates the kinematics and dynamics of a rigid spacecraft suffering from actuator fault, misalignment and bounded external disturbances. The preliminary assumptions are also listed in this section. Section III presents prescribed performance, CA technique and controller design process. Numerical simulations are conducted in Section IV to verify the effectiveness of proposed controller. Finally, the conclusion is given in Section V.

## 2. Preliminaries

### 2.1. Kinematics

The attitude of spacecraft is represented by the nonsingular unit quaternion  $\mathbf{Q} = [q_0, \mathbf{q}_v^T]^T = [q_0, q_1, q_2, q_3]^T \in \mathbb{R}^4$ . Then the kinematics is expressed by:

$$\begin{bmatrix} \dot{q}_0 \\ \dot{\mathbf{q}}_v \end{bmatrix} = \frac{1}{2} \begin{bmatrix} -\mathbf{q}_v^T \\ q_0 \mathbf{I}_3 + \mathbf{q}_v^\times \end{bmatrix} \boldsymbol{\omega} \quad (1)$$

where  $\mathbf{I}_3 \in \mathbb{R}^{3 \times 3}$  is the 3-by-3 identity matrix,  $\boldsymbol{\omega} \in \mathbb{R}^3$  is the angular velocity of the spacecraft body frame  $\mathcal{F}_B$  with respect to the inertia frame  $\mathcal{F}_I$  and expressed in  $\mathcal{F}_B$ . The operator “ $(\cdot)^\times$ ” generates a skew-symmetric matrix to express the cross product of two vectors  $\mathbf{a}$  and  $\mathbf{b}$  by  $\mathbf{a} \times \mathbf{b} = \mathbf{a}^\times \mathbf{b}$ .

To formulate the attitude tracking problem, a virtual spacecraft with the attitude of  $\mathbf{Q}_d = [q_{d0}, \mathbf{q}_{dv}^T]^T \in \mathbb{R}^4$  and angular velocity  $\boldsymbol{\omega}_d \in \mathbb{R}^3$  is assumed to be the target. Similar to (1), the kinematics of the target spacecraft is given by:

$$\begin{bmatrix} \dot{q}_{d0} \\ \dot{\mathbf{q}}_{dv} \end{bmatrix} = \frac{1}{2} \begin{bmatrix} -\mathbf{q}_{dv}^T \\ q_{d0} \mathbf{I}_3 + \mathbf{q}_{dv}^\times \end{bmatrix} \boldsymbol{\omega}_d \quad (2)$$

To describe the discrepancy between the actual unit-quaternion  $\mathbf{Q}$  and the target unit-quaternion  $\mathbf{Q}_d$ , the quaternion error  $\mathbf{Q}_e = [q_{e0}, \mathbf{q}_{ev}^T]^T \in \mathbb{R}^4$  is given by:

$$\mathbf{Q}_e = \mathbf{Q}_d^{-1} \circ \mathbf{Q} = \begin{bmatrix} q_{d0} & \mathbf{q}_{dv}^T \\ -\mathbf{q}_{dv} & q_{d0}\mathbf{I}_3 - \mathbf{q}_{dv}^\times \end{bmatrix} \begin{bmatrix} q_0 \\ \mathbf{q}_v \end{bmatrix} \quad (3)$$

where  $\mathbf{Q}_d^{-1}$  is the conjugate quaternion of  $\mathbf{Q}_d$  and “ $\circ$ ” represents the quaternion multiplication.

Then the error quaternion dynamics is given by [30]:

$$\begin{bmatrix} \dot{q}_{e0} \\ \dot{\mathbf{q}}_{ev} \end{bmatrix} = \frac{1}{2} \begin{bmatrix} -\mathbf{q}_{ev}^T \\ q_{e0}\mathbf{I}_3 + \mathbf{q}_{ev}^\times \end{bmatrix} \boldsymbol{\omega}_e \quad (4)$$

with  $\boldsymbol{\omega}_e = \boldsymbol{\omega} - \mathbf{R}(\mathbf{Q}_e)\boldsymbol{\omega}_d$ .

The relationship between the transformation matrix  $\mathbf{R}$  from  $\mathcal{F}_I$  to  $\mathcal{F}_B$  and the unit quaternion  $\mathbf{Q}$  is:

$$\mathbf{R}(\mathbf{Q}) = (q_0^2 - \mathbf{q}_v^T \mathbf{q}_v) \mathbf{I}_3 + 2\mathbf{q}_v \mathbf{q}_v^T - 2q_0 \mathbf{q}_v^\times \quad (5)$$

## 2.2. Dynamics

The dynamics of the attitude motion of a rigid spacecraft is expressed as [31]:

$$\mathbf{J}\dot{\boldsymbol{\omega}} = -\boldsymbol{\omega}^\times \mathbf{J}\boldsymbol{\omega} + \mathbf{D}\mathbf{U}_r + \mathbf{d} \quad (6)$$

where  $\mathbf{J} = \mathbf{J}^T \in \mathbb{R}^{3 \times 3}$  denotes inertial matrix of the spacecraft,  $\mathbf{D} \in \mathbb{R}^{3 \times N}$  ( $N$  is the number of actuators) is the torque distribution matrix,  $\mathbf{U}_r \in \mathbb{R}^N$  is the output control torque generated by the actuators and  $\mathbf{d} \in \mathbb{R}^3$  is the external disturbance. To guarantee the 3-axis controllability of the spacecraft, more than 3 non-coplanar mounted actuators are essential and the matrix  $\mathbf{D}$  is full row rank as a consequence, i.e.,  $\text{rank}(\mathbf{D}) = 3$ .

For the fault-free cases, the output control torque  $\mathbf{U}_r = [u_{r1}, u_{r2}, \dots, u_{rN}]^T$  equals to the allocated value  $\mathbf{U}_a = [u_{a1}, u_{a2}, \dots, u_{aN}]^T$  via a specific control allocation technique. When the actuator faults or failures occur, actuators can not produce the exact control torque allocated to them and the real output is

proportional to the allocated value  $\mathbf{U}_a$  with an effectiveness gain. Then we have:

$$\mathbf{U}_r = \mathbf{E}(t) \mathbf{U}_a \quad (7)$$

where  $\mathbf{E}(t) = \text{diag}([e_1(t), e_2(t), \dots, e_N(t)]) \in \mathbb{R}^{N \times N}$  is the effectiveness gain matrix. The elements  $e_i(t) (i = 1, 2, \dots, N)$  are in the interval  $[0, 1]$ . Note that the case  $e_i(t) = 0$  indicates that the  $i$ th actuator generates zero output torque according to  $u_{r_i} = e_i(t)u_{a_i}$ . In such a situation, the  $i$ th actuator undergoes a complete failure.  $0 < e_i(t) < 1$  implies that the  $i$ th actuator partially loses its effectiveness and generates a smaller control torque. When  $e_i(t) = 1$ ,  $i$ th actuator works normally and the actual output torque  $u_{r_i}$  equals to the allocated value  $u_{a_i}$ .

When the actuators' working condition changes,  $e_i(t)$  may change accordingly. Thus  $e_i(t)$  should be estimated by a proper fault detection and diagnosis (FDD) mechanism in real time. The estimated value is denoted as  $\hat{e}_i(t)$  and the estimation error is defined as  $\tilde{e}_i$  with  $\tilde{e}_i = \hat{e}_i(t) - e_i(t) = \delta_{e_i}(t)\hat{e}_i(t) (\hat{e}_i(t) \neq 0)$ . Thus equation (7) can be further written as:

$$\mathbf{U}_r = (\mathbf{I}_n - \Delta\mathbf{E}) \hat{\mathbf{E}}(t) \mathbf{U}_a \quad (8)$$

where  $\Delta\mathbf{E} = \text{diag}([\delta_{e_1}(t), \delta_{e_2}(t), \dots, \delta_{e_N}(t)])$ . In order to optimize the torque distribution strategy taking the actuators' effectiveness into consideration and develop robust controller incorporating control allocation,  $\mathbf{E}(t)$  should be suitably estimated and accurate enough, i.e.  $\hat{e}_i(t) \approx e_i(t)$ ,  $\tilde{e}_i = \hat{e}_i(t) - e_i(t) = \delta_{e_i}(t)\hat{e}_i(t) \approx 0$ . Thus each component of  $\delta_{e_i}(t) \approx 0 \ll 1$ . Consequently,  $\Delta\mathbf{E}$  is upper bounded, and the upper bound of matrix  $\Delta\mathbf{E}$  is defined as  $\Delta_E$ , i.e.  $\|\Delta\mathbf{E}\| \leq \Delta_E \ll 1$ .

For the case  $\hat{e}_i(t) = 0$ ,  $\delta_{e_i}(t) = 0$  is defined. Then equation (8) and the upper bound of  $\|\Delta\mathbf{E}\| \leq \Delta_E \ll 1$  are still valid.

In addition, when the misalignment of the actuators is considered, the torque distribution matrix should be modified as:

$$\mathbf{D} = \mathbf{D}_n - \Delta\mathbf{D} \quad (9)$$

where  $\mathbf{D}_n$  is the nominal torque distribution matrix and  $\Delta\mathbf{D}$  is the unknown constant misalignment matrix. Since the installation should be with certain accuracy,  $\Delta\mathbf{D}$  representing the misalignment is also assumed to be bounded with  $\|\Delta\mathbf{D}\| \leq \Delta_D \ll 1$ .

Substituting equation (8) and (9) into (6), the dynamics equation of the spacecraft considering unknown misalignment and actuator faults is given by:

$$\begin{aligned} \mathbf{J}\dot{\boldsymbol{\omega}} &= -\boldsymbol{\omega}^\times\mathbf{J}\boldsymbol{\omega} + (\mathbf{D}_n - \Delta\mathbf{D})(\mathbf{I}_n - \Delta\mathbf{E}(t))\hat{\mathbf{E}}(t)\mathbf{U}_a + \mathbf{d} \\ &= -\boldsymbol{\omega}^\times\mathbf{J}\boldsymbol{\omega} + \mathbf{D}_n\hat{\mathbf{E}}(t)\mathbf{U}_a - \mathbf{L}\hat{\mathbf{E}}(t)\mathbf{U}_a + \mathbf{d} \end{aligned} \quad (10)$$

where  $\mathbf{L} = \Delta\mathbf{D} + \mathbf{D}_n\Delta\mathbf{E}(t) - \Delta\mathbf{D}\Delta\mathbf{E}(t)$  and  $\|\mathbf{L}\| \leq \bar{l} \ll 1$ .

To facilitate control system design, the following assumption are used in the following subsequent developments.

**Assumption 1.** *The inertia matrix  $\mathbf{J}$  is a symmetric, positive definite and upper bounded, i.e.  $\|\mathbf{J}\| \leq \bar{J}$  with  $\bar{J}$  being a positive constant.*

**Assumption 2.** *The angular velocity of the target spacecraft and its time derivative is bounded, namely  $\|\boldsymbol{\omega}_d\| \leq \bar{\omega}$  and  $\|\dot{\boldsymbol{\omega}}_d\| \leq \bar{\omega}$ , which means the spacecraft is expected to track a continuously smooth attitude trajectory.*

**Assumption 3.** *The external disturbance  $\mathbf{d}$  is bounded such that  $\|\mathbf{d}\| \leq \bar{d}$  with  $\bar{d}$  being a positive constant.*

**Assumption 4.** *The lumped uncertainty matrix is assumed to be bounded, i.e.  $\|\mathbf{L}\| \leq \bar{l} \ll 1$ , with  $\|\Delta\mathbf{D}\| \leq \Delta_D \ll 1$ ,  $\|\Delta\mathbf{E}\| \leq \Delta_E \ll 1$ , and  $\Delta_D$ ,  $\Delta_E$  and  $\bar{l}$  are positive constants. This assumption is reasonable since the initial installation and the fault estimation should be with certain accuracy.*

**Assumption 5.** *The maximum number of actuators suffer from total failures simultaneously is smaller than  $N - 3$ , and the rank of matrix  $\mathbf{E}(t)$  and  $\hat{\mathbf{E}}(t)$  is larger than 3, i.e.  $\text{rank}(\mathbf{E}(t)) \geq 3$  and  $\text{rank}(\hat{\mathbf{E}}(t)) \geq 3$ . The matrix  $\mathbf{D}\hat{\mathbf{E}}(t)^3\mathbf{D}^T$  is also assumed to be invertible, i.e.  $\det(\mathbf{D}\hat{\mathbf{E}}(t)^3\mathbf{D}^T) \neq 0$ . This assumption guarantees the 3-axis controllability and solids the foundation to develop FT control strategy [19, 20].*

### 3. Controller Design

In this section, we present the major issues considered in this paper such as the guaranteed prescribed performance and minimizing the use of the faulty actuator. Then a robust adaptive sliding mode controller is developed to complete the attitude tracking. The control objective of this paper can be summarized as follows:

- 1 .  $\lim_{t \rightarrow \infty} \mathbf{q}_e(t) \rightarrow 0$ , and  $\mathbf{q}_e(t)$  is bounded during the control process by some monotonically decreasing time-varying function  $f(t)$  as the prescribed performance constraint, i.e.  $|\mathbf{q}_e(t)| < f(t)$ .
2. The control signal allocated to the  $i$ th actuator  $u_{ai}$  is to be minimized according to the estimated effectiveness of the actuator  $\hat{e}_i$ , i.e.  $\min \mathbf{U}_a^T \hat{\mathbf{E}}(t)^{-1} \mathbf{U}_a$ , subject to  $\mathbf{D}_n \hat{\mathbf{E}}(t) \mathbf{U}_a = \mathbf{U}_c$ .

#### 3.1. Prescribed performance

Prescribed performance means that the tracking error converges to a pre-defined arbitrarily small residual set, with convergence rate no less than a prescribed value, exhibiting maximum overshoot as well as undershoot less than some sufficiently small preassigned constant [24, 25]. To guarantee the prescribed performance, a performance function is introduced as:

$$\rho(t) = (\rho(0) - \rho(\infty)) e^{-\mu t} + \rho(\infty) \quad (11)$$

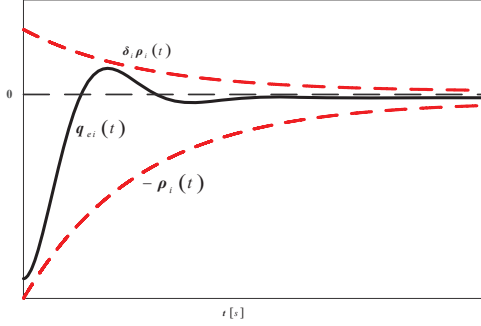
where  $\rho(0)$  is the initial value of  $\rho(t)$ ,  $\rho(\infty) > 0$  is the limit of  $\rho(t)$  when  $t$  goes to infinity, i.e.  $\rho(\infty) = \lim_{t \rightarrow \infty} \rho(t) > 0$ , and  $\mu > 0$  describes the convergence rate of  $\rho(t)$ .

For the unit quaternion error given by (4), guaranteed prescribed performance requires that:

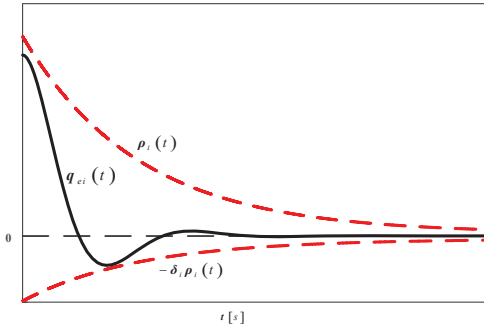
$$-\rho_i(t) < q_{ei}(t) < \delta_i \rho_i(t) \quad q_{ei}(0) < 0 \quad (12a)$$

$$-\delta_i \rho_i(t) < q_{ei}(t) < \rho_i(t) \quad q_{ei}(0) \geq 0 \quad (12b)$$

where the subscript  $i = 1, 2, 3$  represents the  $i$ th component, and  $q_{ei}$  is the  $i$ th component of  $\mathbf{q}_e$ ,  $\delta_i \in [0, 1]$  governs the maximum overshoot together with  $\rho_i(t)$ . These statements can be clearly described as in Fig. 1.



(a) Eqn (12a)



(b) Eqn (12b)

Figure 1: Tracking error prescribed performance

To unify the prescribed performance relationship (12), a zero crossing comparator is developed as:

$$\eta(q_{ei}(0)) = \begin{cases} 1 & q_{ei}(0) \geq 0 \\ 0 & q_{ei}(0) < 0 \end{cases} \quad (13)$$

For simplicity,  $\eta_i(q_{ei}(0))$  is denoted as  $\eta_i$  for short.

With this zero crossing comparator, two parameters are further defined:

$$\begin{cases} \varepsilon_{li}(t) = \eta_i \delta_i + (1 - \eta_i) \\ \varepsilon_{ui}(t) = \eta_i + (1 - \eta_i) \delta_i \end{cases} \quad (14)$$

Then equation (12) can be rewritten as:

$$-\varepsilon_{li}\rho_i(t) < q_{ei}(t) < \varepsilon_{ui}\rho_i(t) \quad (15)$$

It is known that both the convergence rate and overshoot as well as undershoot can be guaranteed if the tracking error is controlled to behave and evolve according to (15). However, it is difficult to develop controller and conduct stability analysis. Thus a state variable transformation is introduced as in [26, 32]:

$$q_{ei}(t) = T_i(v_i)\rho_i(t) \quad (16)$$

where  $v_i$  is the new transformed unconstrained state and the function  $T_i(v_i)$  is given by:

$$T_i(v_i) = \frac{\varepsilon_{ui}e^{(v_i+r_i)} - \varepsilon_{li}e^{-(v_i+r_i)}}{e^{(v_i+r_i)} + e^{-(v_i+r_i)}} \quad (17)$$

with  $r_i = \frac{1}{2} \ln \left( \frac{\varepsilon_{li}}{\varepsilon_{ui}} \right)$ .

**Property 1.** Consider the state transformation function (17), the following property hold:

- $T_i(v_i)$  is both lower and upper bounded and it satisfies the inequality  $-\varepsilon_{li} < T_i(v_i) < \varepsilon_{ui}$ ;
- $T_i(v_i)$  is differentiable and its derivation is bounded, i.e.  $0 < \frac{dT_i(v_i)}{dv_i} = \frac{2(\varepsilon_{ui} + \varepsilon_{li})}{e^{2(v_i+r_i)} + e^{-2(v_i+r_i)} + 2} \leq \frac{\varepsilon_{ui} + \varepsilon_{li}}{2}$ ;
- $T_i(v_i)$  is monotone increasing, and  $\lim_{v_i \rightarrow -\infty} T_i(v_i) = -\varepsilon_{li}$ ,  $\lim_{v_i \rightarrow \infty} T_i(v_i) = \varepsilon_{ui}$  and  $\lim_{v_i \rightarrow 0} T_i(v_i) = 0$ .

According to the property 1,  $T_i(v_i)$  is invertible and  $v_i = T_i^{-1}(\lambda_i(t))$  is given by:

$$v_i = \frac{1}{2} \ln (\varepsilon_{ui}\lambda_i(t) + \varepsilon_{ui}\varepsilon_{li}) - \frac{1}{2} \ln (\varepsilon_{ui}\varepsilon_{li} - \varepsilon_{li}\lambda_i(t)) \quad (18)$$

with  $\lambda_i(t) = \frac{q_{ei}(t)}{\rho_i(t)}$ .

By using the transformation (17), the lower bound and upper bound imposed on  $q_{ei}(t)$  in (12) is converted to the unconstrained relation (17). Therefore, the

prescribed performance requirement is converted to control the signal  $v$  to be bounded and converge to a small residual set since  $v_i \rightarrow 0$  is equivalent to  $q_{ei} \rightarrow 0$ .

### 3.2. Control allocation technique

FT control strategies depend on the existence of the system redundancy [14] and the control effect of such strategies is closely related to the effectiveness of the actuators. Thus the control effectiveness of the actuator and the control allocation method should be considered in the controller design. When the effectiveness matrix  $\mathbf{E}(t)$  is estimated by a proper FDD mechanism, the control torque should be reallocated subject to some optimization performance index, such as minimize the use of faulty actuators according to the properly estimated effectiveness[19, 20]. In such cases, the control allocation is changed to a  $L_2$ -optimization problem:

$$\begin{aligned} & \min \quad \mathbf{U}_a^T \hat{\mathbf{E}}(t)^{-1} \mathbf{U}_a \\ & \text{subject to} \quad \mathbf{D}_n \hat{\mathbf{E}}(t) \mathbf{U}_a = \mathbf{U}_c \end{aligned} \quad (19)$$

where  $\mathbf{U}_c$  is the control command generated by the controller.

It is clear that when  $e_i(t) \rightarrow 0$ ,  $e_i^{-1}(t) \rightarrow \infty$ . To optimize the index  $u_{ai}^T \hat{e}_i^{-1} u_{ai}$ , which is equivalent to optimize  $u_{ai}^T e_i^{-1} u_{ai}$  when  $e_i(t)$  is properly estimated as  $\hat{e}_i(t)$ ,  $u_{ai}$  is required to go to zero, i.e.  $u_{ai} \rightarrow 0$  when  $e_i(t) \rightarrow 0$ . Thus the CA method minimizes the use of the faulty actuator using the estimated effectiveness matrix  $\hat{\mathbf{E}}(t)$ , which is desirable in practical space missions.

Solving the optimization problem, one can obtain the solution as:

$$\mathbf{U}_a = \hat{\mathbf{E}}^2(t) \mathbf{D}_n^T \left( \mathbf{D}_n \hat{\mathbf{E}}^3(t) \mathbf{D}_n^T \right)^{-1} \mathbf{U}_c \quad (20)$$

Substituting equation (20) into (10), the dynamics is further written as:

$$\mathbf{J}\dot{\boldsymbol{\omega}} = -\boldsymbol{\omega}^\times \mathbf{J}\boldsymbol{\omega} + \mathbf{U}_c - \mathbf{L}\mathbf{D}^\# \mathbf{U}_c + \mathbf{d} \quad (21)$$

with  $\mathbf{D}^\# = \hat{\mathbf{E}}^3(t) \mathbf{D}^T \left( \mathbf{D} \hat{\mathbf{E}}^3(t) \mathbf{D}^T \right)^{-1}$ ,  $\mathbf{D}^\#$  is upper bounded and  $\|\mathbf{D}^\#\| \leq \bar{D}$  with  $\bar{D}$  being a finite positive constant. This property can also be found in [19] and [20].

### 3.3. Controller design

In this subsection, we will develop a robust adaptive sliding mode controller to stabilize the transformed error  $v$  given by (18). The whole loop control schematic diagram is shown in Fig. 2.

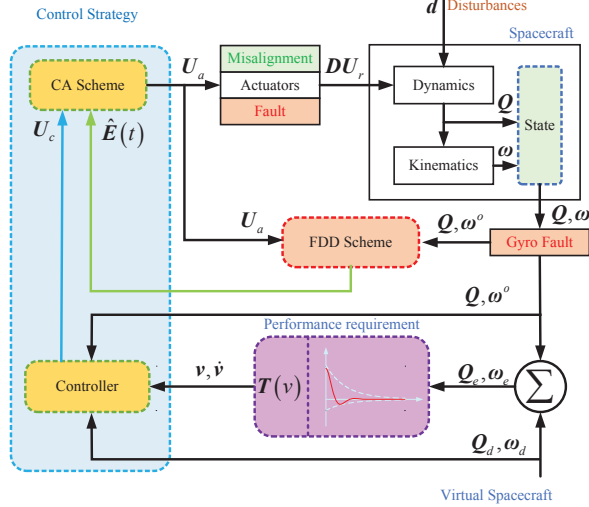


Figure 2: Whole loop control schematic diagram

Figure 2 presents the whole loop of spacecraft attitude control system where, the solid line rectangle block are physical instrument, such as the actuators, spacecraft basement and sensors, and the dashed line rectangle blocks are virtual computation unit, such as the control strategy and performance requirement. The actuator fault, misalignment and various disturbance are considered in establishing the dynamic equation (10). The gyro fault only influence the measured angular velocity for feedback and affect the control effect. The discrepancy between the measured angular velocity and its true value can be caused by gyro fault or adversarial sensor attack. This fault can be modelled as in [21]:

$$\boldsymbol{\omega}^o = \boldsymbol{\omega} + \mathbf{W}(t, \boldsymbol{\omega}) \quad (22)$$

where  $\mathbf{W}(t) = [\delta_{\omega_1}(t, \omega_1), \delta_{\omega_2}(t, \omega_2), \delta_{\omega_3}(t, \omega_3)]^T$  and  $\boldsymbol{\omega}^o$  is the measured an-

gular velocity for feedback.  $\mathbf{W}(t)$  is bounded by  $\|\mathbf{W}(t)\| \leq \bar{W}$ . It is clear that the uncompromised angular velocity  $\omega_i$  is corrupted with a faulty signal  $\delta\omega_i(t, \omega_i) (i = 1, 2, 3)$ . In this paper, the time derivative of  $\mathbf{W}$  is also assumed to be bounded, i.e.  $\|\dot{\mathbf{W}}\| \leq \bar{W}_d$ [21]. The cases where  $\dot{\mathbf{W}}$  is unbounded will be our future work.

According to the definition, we can get the following relationship by the triangle inequality:

$$\|\boldsymbol{\omega}\| = \|\boldsymbol{\omega}^o - \mathbf{W}(t, \boldsymbol{\omega})\| \leq \|\boldsymbol{\omega}^o\| + \bar{W} \quad (23)$$

Before we move forward to the controller design, we establish some useful inequalities as follows:

$$\|\boldsymbol{\omega}_e\| = \|\boldsymbol{\omega} - \mathbf{R}(\mathbf{Q}_e)\boldsymbol{\omega}_d\| \leq (\bar{\omega} + \bar{W}) + \|\boldsymbol{\omega}^o\| \quad (24a)$$

$$\|\boldsymbol{\omega}_e^o\| = \|\boldsymbol{\omega}^o - \mathbf{R}(\mathbf{Q}_e)\boldsymbol{\omega}_d\| \leq \bar{\omega} + \|\boldsymbol{\omega}^o\| \leq \bar{\omega}_e \quad (24b)$$

$$\|(\mathbf{R}(\mathbf{Q}_e)\boldsymbol{\omega}_d)^\times \mathbf{J}\boldsymbol{\omega}\| \leq \bar{J}\bar{\omega}\bar{W} + \bar{J}\bar{\omega}\|\boldsymbol{\omega}^o\| \quad (24c)$$

$$\|\mathbf{J}\boldsymbol{\omega}_e^\times \mathbf{R}(\mathbf{Q}_e)\boldsymbol{\omega}_d\| \leq (\bar{J}\bar{\omega}^2 + \bar{J}\bar{\omega}\bar{W}) + \bar{J}\bar{\omega}\|\boldsymbol{\omega}^o\| \quad (24d)$$

$$\|-\mathbf{J}\mathbf{R}(\mathbf{Q}_e)\dot{\boldsymbol{\omega}}_d\| \leq \bar{J}\dot{\omega} \quad (24e)$$

$$\|\boldsymbol{\omega}_e^{o\times} \mathbf{J}\mathbf{W}\| \leq \bar{J}\bar{\omega}\bar{W} + \bar{J}\bar{W}\|\boldsymbol{\omega}^o\| \quad (24f)$$

where  $\bar{\omega}_e$  is the upper bound of  $\bar{\omega} + \|\boldsymbol{\omega}^o\|$  as shown in (24b).

A lumped nonlinear function is defined as:

$$\begin{aligned} \mathbf{f} = & -(\mathbf{R}(\mathbf{Q}_e)\boldsymbol{\omega}_d)^\times \mathbf{J}\boldsymbol{\omega} + \mathbf{W}^\times \mathbf{J}\mathbf{W} + \mathbf{J}\boldsymbol{\omega}_e^\times \mathbf{R}(\mathbf{Q}_e)\boldsymbol{\omega}_d \\ & - \mathbf{J}\mathbf{R}(\mathbf{Q}_e)\dot{\boldsymbol{\omega}}_d + \mathbf{J}\dot{\mathbf{W}} + \boldsymbol{\omega}_e^{o\times} \mathbf{J}\mathbf{W} + \mathbf{d} \end{aligned} \quad (25)$$

According to the inequalities of (24), the lumped nonlinear function is upper bounded:

$$\begin{aligned}\|f\| &\leq \left( 3\bar{J}\bar{\omega}\bar{W} + \bar{J}\bar{\omega}^2 + \bar{J}\bar{W}^2 + \bar{J}\dot{\omega} + \bar{J}\bar{W}_d + \bar{d} \right) \\ &\quad + (2\bar{J}\bar{\omega} + \bar{J}\bar{W}) \|\boldsymbol{\omega}^o\| \\ &= c_1 + c_2 \|\boldsymbol{\omega}^o\| \leq \bar{f}\end{aligned}\tag{26}$$

with  $c_1 = 3\bar{J}\bar{\omega}\bar{W} + \bar{J}\bar{\omega}^2 + \bar{J}\bar{W}^2 + \bar{J}\dot{\omega} + \bar{J}\bar{W}_d + \bar{d}$  and  $c_2 = 2\bar{J}\bar{\omega} + \bar{J}\bar{W}$ .

Then we substitute  $\boldsymbol{\omega}_e^o = \boldsymbol{\omega}^o - \mathbf{R}(\mathbf{Q}_e)\boldsymbol{\omega}_d$  into (21) and obtain:

$$\begin{aligned}\mathbf{J}\dot{\boldsymbol{\omega}}_e^o &= -\boldsymbol{\omega}_e^{o\times}\mathbf{J}\boldsymbol{\omega}^o + \mathbf{U}_c - \mathbf{L}\mathbf{D}^\# \mathbf{U}_c + \boldsymbol{\omega}_e^{o\times}\mathbf{J}\mathbf{W} \\ &\quad - (\mathbf{R}(\mathbf{Q}_e)\boldsymbol{\omega}_d)^\times\mathbf{J}\boldsymbol{\omega} + \mathbf{W}^\times\mathbf{J}\mathbf{W} + \mathbf{J}\boldsymbol{\omega}_e^{o\times}\mathbf{R}(\mathbf{Q}_e)\boldsymbol{\omega}_d \\ &\quad - \mathbf{J}\mathbf{R}(\mathbf{Q}_e)\dot{\boldsymbol{\omega}}_d + \mathbf{J}\dot{\mathbf{W}} + \mathbf{d} \\ &= -\boldsymbol{\omega}_e^{o\times}\mathbf{J}\boldsymbol{\omega}^o + \mathbf{U}_c - \mathbf{L}\mathbf{D}^\# \mathbf{U}_c + \mathbf{f}\end{aligned}\tag{27}$$

where  $\mathbf{L}\mathbf{D}^\#$  is upper bounded with  $\|\mathbf{L}\mathbf{D}^\#\| \leq \bar{l}\bar{D} = c_3$ . To theoretically guarantee the stability,  $c_3 < 1$  is required for the most conservative case. In this paper, we assume  $c_3 < 1$  and this assumption is verified in the simulation. The graph of  $\|\mathbf{L}\mathbf{D}^\#\|$  during the simulation is added as Fig. 15 in the supporting information.

Then a robust adaptive sliding mode control strategy is proposed. The sliding surface is developed as:

$$\mathbf{S} = \boldsymbol{\omega}_e^o + k\mathbf{v}\tag{28}$$

The controller is designed as:

$$\mathbf{U}_c = \mathbf{U}_{c_1} + \mathbf{U}_{c_2}\tag{29}$$

$$\mathbf{U}_{c_1} = -k_1\mathbf{S} - k_2\mathbf{v} + \mathbf{U}_{c_1}^{com}\tag{30}$$

with

$$\mathbf{U}_{c_1}^{com} = \begin{cases} \mathbf{0} & \|\mathbf{S}\| = 0 \\ \left[ k\boldsymbol{\omega}_e^{oT}(\mathbf{J}\boldsymbol{\omega}^o)^\times\mathbf{v} + k\boldsymbol{\omega}_e^{oT}\mathbf{J}\dot{\mathbf{v}} \right] \frac{\mathbf{S}}{\mathbf{S}^T\mathbf{S}} & \|\mathbf{S}\| \neq 0 \end{cases}\tag{31}$$

and

$$\mathbf{U}_{c_2} = \begin{cases} -\frac{1}{1-c_3} \frac{\mathbf{S}}{\|\mathbf{S}\|} \hat{u} & \hat{u} \|\mathbf{S}\| \geq \varepsilon \\ -\frac{1}{1-c_3} \frac{\mathbf{S}}{\varepsilon} \hat{u}^2 & \hat{u} \|\mathbf{S}\| < \varepsilon \end{cases} \quad (32)$$

with

$$\hat{\mathbf{u}} = \hat{c}_1 + \hat{c}_2 \|\boldsymbol{\omega}^o\| + \hat{c}_3 \|\mathbf{U}_{c_1}\| \quad (33)$$

where  $\hat{c}_1$ ,  $\hat{c}_2$  and  $\hat{c}_3$  are given by the following adaptive law:

$$\begin{cases} \dot{\hat{c}}_1 = p_1 (-\varepsilon_1 \hat{c}_1 + \|\mathbf{S}\|) \\ \dot{\hat{c}}_2 = p_2 (-\varepsilon_2 \hat{c}_2 + \|\mathbf{S}\| \|\boldsymbol{\omega}^o\|) \\ \dot{\hat{c}}_3 = p_3 (-\varepsilon_3 \hat{c}_3 + \|\mathbf{S}\| \|\mathbf{U}_{c_1}\|) \end{cases} \quad (34)$$

In controller (28) to (34),  $k$ ,  $k_1$ ,  $k_2$ ,  $p_1$ ,  $p_2$ ,  $p_3$ ,  $\varepsilon_1$ ,  $\varepsilon_2$ ,  $\varepsilon_3$  are positive.

Then the robust prescribed performance guaranteed FT adaptive sliding mode control can be concluded by the following theorem:

**Theorem 1.** Consider the relative kinematics equation (4), relative dynamics equation (27) with actuator fault and misalignment as described in (8) and (9), the prescribed performance requirement (15) under the assumptions 1 to 5. If the system is controlled by the controller (28) to (33) with the control gains being updated by the adaptive law (34), then the actuator fault, misalignment, estimation error of FDD scheme and external disturbance are accommodated automatically and prescribed performance of the tracking error is guaranteed. More specifically, the measured angular velocity error  $\boldsymbol{\omega}_e^o$ , the transformed state  $\mathbf{v}$  and the estimation error  $\tilde{c}_1 = c_1 - \hat{c}_1$ ,  $\tilde{c}_2 = c_2 - \hat{c}_2$ ,  $\tilde{c}_3 = c_3 - \hat{c}_3$  are controlled to be ultimately uniformly bounded (UUB).

**Property 2.** Consider the adaptive law (34). If the initial value of  $\hat{c}_1(t)$ ,  $\hat{c}_2(t)$  and  $\hat{c}_3(t)$  are chosen to be positive number,  $\hat{c}_1(t)$ ,  $\hat{c}_2(t)$  and  $\hat{c}_3(t)$  will be positive for all the time, and  $\hat{u}(t)$  will also be positive for all the time.

This property can be easily proved by solving the differential equation (34). The solutions are given by  $\hat{c}_1(t) = \hat{c}_1(0) e^{-p_1 \varepsilon_1 t} + \|\mathbf{S}\| / p_1 \varepsilon_1 > 0$  when  $\hat{c}_1(0) > 0$ ,  $\hat{c}_2(t) = \hat{c}_2(0) e^{-p_2 \varepsilon_2 t} + \|\mathbf{S}\| \cdot \|\boldsymbol{\omega}^o\| / p_2 \varepsilon_2 > 0$  when  $\hat{c}_2(0) > 0$ , and  $\hat{c}_3(t) = \hat{c}_3(0) e^{-p_3 \varepsilon_3 t} + \|\mathbf{S}\| \cdot \|\mathbf{U}_{c_1}\| / p_3 \varepsilon_3 > 0$  when  $\hat{c}_3(0) > 0$ . Then  $\hat{\mathbf{u}} = \hat{c}_1 + \hat{c}_2 \|\boldsymbol{\omega}^o\| + \hat{c}_3 \|\mathbf{U}_{c_1}\|$  will always be positive when  $\hat{c}_1(t)$ ,  $\hat{c}_2(t)$  and  $\hat{c}_3(t)$  are positive.

*Proof.* To prove the stability, a Lyapunov candidate is firstly chosen as:

$$V_1 = \frac{1}{2} \mathbf{S}^T \mathbf{J} \mathbf{S} + \frac{1}{2} k^2 \mathbf{v}^T \mathbf{J} \mathbf{v} \quad (35)$$

The time derivative of  $V_1$  is obtained as:

$$\begin{aligned} \dot{V}_1 &= \mathbf{S}^T \mathbf{J} \dot{\mathbf{S}} + k^2 \mathbf{v}^T \mathbf{J} \dot{\mathbf{v}} \\ &= \mathbf{S}^T (-\omega_e^{o \times} \mathbf{J} \boldsymbol{\omega}^o + \mathbf{f} + \mathbf{U}_c - \mathbf{L} \mathbf{D}^\# \mathbf{U}_c - k \mathbf{J} \dot{\mathbf{v}}) + k^2 \mathbf{v}^T \mathbf{J} \dot{\mathbf{v}} \\ &= \mathbf{S}^T (\mathbf{f} + \mathbf{U}_c - \mathbf{L} \mathbf{D}^\# \mathbf{U}_c) - k \boldsymbol{\omega}_e^{o T} (\mathbf{J} \boldsymbol{\omega}^o)^\times \mathbf{v} - k \boldsymbol{\omega}_e^{o T} \mathbf{J} \dot{\mathbf{v}} \end{aligned} \quad (36)$$

Then the proof will be separated into two cases: Case I.  $\|\mathbf{S}\| \neq 0$  and Case II.  $\|\mathbf{S}\| = 0$ .

**Case I.**  $\|\mathbf{S}\| \neq 0$

In this case, substituting (29), (36) can be further written into:

$$\begin{aligned} \dot{V}_1 &= \mathbf{S}^T \left( \mathbf{U}_{c_1} - \left[ k \boldsymbol{\omega}_e^{o T} (\mathbf{J} \boldsymbol{\omega}^o)^\times \mathbf{v} + k \boldsymbol{\omega}_e^{o T} \mathbf{J} \dot{\mathbf{v}} \right] \frac{\mathbf{S}}{\|\mathbf{S}\|} \right) \\ &\quad + \mathbf{S}^T (\mathbf{f} + \mathbf{U}_{c_2} - \mathbf{L} \mathbf{D}^\# \mathbf{U}_{c_1} - \mathbf{L} \mathbf{D}^\# \mathbf{U}_{c_2}) \end{aligned} \quad (37)$$

Substituting  $\mathbf{U}_{c_1}$  into (37), one obtains:

$$\begin{aligned} \dot{V}_1 &= -k_1 \mathbf{S}^T \mathbf{S} - k k_2 \mathbf{v}^T \mathbf{v} - k_2 \boldsymbol{\omega}_e^{o T} \mathbf{v} \\ &\quad + \mathbf{S}^T (\mathbf{f} - \mathbf{L} \mathbf{D}^\# \mathbf{U}_{c_1} + \mathbf{U}_{c_2} - \mathbf{L} \mathbf{D}^\# \mathbf{U}_{c_2}) \end{aligned} \quad (38)$$

According to (28), it is clear that:

$$\mathbf{S}^T \mathbf{S} = \boldsymbol{\omega}_e^{o T} \boldsymbol{\omega}_e^o + k^2 \mathbf{v}^T \mathbf{v} + 2k \boldsymbol{\omega}_e^{o T} \mathbf{v} \geq 2k \|\boldsymbol{\omega}_e^{o T} \mathbf{v}\| \quad (39)$$

Then we obtain

$$\begin{aligned} \dot{V}_1 &\leq - \left( k_1 - \frac{k_2}{2k} \right) \mathbf{S}^T \mathbf{S} - k k_2 \mathbf{v}^T \mathbf{v} \\ &\quad + \mathbf{S}^T (\mathbf{f} - \mathbf{L} \mathbf{D}^\# \mathbf{U}_{c_1} + \mathbf{U}_{c_2} - \mathbf{L} \mathbf{D}^\# \mathbf{U}_{c_2}) \end{aligned} \quad (40)$$

To handle the lumped nonlinear function  $\mathbf{f}$  and the remaining term, a new Lyapunov function is defined as:

$$V_2 = V_1 + \frac{1}{2p_1} \tilde{c}_1^2 + \frac{1}{2p_2} \tilde{c}_2^2 + \frac{1}{2p_3} \tilde{c}_3^2 \quad (41)$$

Taking the time derivatives, we get:

$$\begin{aligned}
\dot{V}_2 &= - \left( k_1 - \frac{k_2}{2k} \right) \mathbf{S}^T \mathbf{S} - kk_2 \mathbf{v}^T \mathbf{v} - \frac{1}{p_1} \tilde{c}_1 \dot{\tilde{c}}_1 - \frac{1}{p_2} \tilde{c}_2 \dot{\tilde{c}}_2 \\
&\quad - \frac{1}{p_3} \tilde{c}_3 \dot{\tilde{c}}_3 + \mathbf{S}^T (\mathbf{f} - \mathbf{L}\mathbf{D}^\# \mathbf{U}_{c_1} + (\mathbf{I}_3 - \mathbf{L}\mathbf{D}^\#) \mathbf{U}_{c_2}) \\
&\leq - \left( k_1 - \frac{k_2}{2k} \right) \mathbf{S}^T \mathbf{S} - kk_2 \mathbf{v}^T \mathbf{v} - \frac{1}{p_1} \tilde{c}_1 \dot{\tilde{c}}_1 - \frac{1}{p_2} \tilde{c}_2 \dot{\tilde{c}}_2 \\
&\quad - \frac{1}{p_3} \tilde{c}_3 \dot{\tilde{c}}_3 + \|\mathbf{S}\| (c_1 + c_2 \|\boldsymbol{\omega}^o\| + c_3 \|\mathbf{U}_{c_1}\|) \\
&\quad + \mathbf{S}^T (\mathbf{I}_3 - \mathbf{L}\mathbf{D}^\#) \mathbf{U}_{c_2}
\end{aligned} \tag{42}$$

Substituting the adaptive law (34) and using  $\hat{c}_i = c_i - \tilde{c}_i (i = 1, 2, 3)$ , we can obtain:

$$\begin{aligned}
\dot{V}_2 &\leq - \left( k_1 - \frac{k_2}{2k} \right) \mathbf{S}^T \mathbf{S} - kk_2 \mathbf{v}^T \mathbf{v} + \varepsilon_1 \tilde{c}_1 \hat{c}_1 + \varepsilon_2 \tilde{c}_2 \hat{c}_2 \\
&\quad + \varepsilon_3 \tilde{c}_3 \hat{c}_3 + \|\mathbf{S}\| (\hat{c}_1 + \hat{c}_2 \|\boldsymbol{\omega}^o\| + \hat{c}_3 \|\mathbf{U}_{c_1}\|) \\
&\quad + \mathbf{S}^T (\mathbf{I}_3 - \mathbf{L}\mathbf{D}^\#) \mathbf{U}_{c_2}
\end{aligned} \tag{43}$$

According to (32), the proof will be conducted for the two scenarios:

a).  $\hat{u} \|\mathbf{S}\| \geq \varepsilon$

In this case, substituting  $\mathbf{U}_{c_2}$  into (43), we obtain:

$$\begin{aligned}
\dot{V}_2 &= - \left( k_1 - \frac{k_2}{2k} \right) \mathbf{S}^T \mathbf{S} - kk_2 \mathbf{v}^T \mathbf{v} - \frac{1}{2} \varepsilon_1 \tilde{c}_1^2 - \frac{1}{2} \varepsilon_2 \tilde{c}_2^2 \\
&\quad - \frac{1}{2} \varepsilon_3 \tilde{c}_3^2 + \frac{1}{2} \varepsilon_1 c_1^2 + \frac{1}{2} \varepsilon_2 c_2^2 + \frac{1}{2} \varepsilon_3 c_3^2 \\
&\quad + \hat{u} \left( \|\mathbf{S}\| - \frac{\mathbf{S}^T (\mathbf{I}_3 - \mathbf{L}\mathbf{D}^\#) \mathbf{S}}{(1 - c_3) \|\mathbf{S}\|} \right)
\end{aligned} \tag{44}$$

For the term, the following inequality holds:

$$\begin{aligned}
\|\mathbf{S}^T (\mathbf{I}_3 - \mathbf{L}\mathbf{D}^\#) \mathbf{S}\| &\geq \mathbf{S}^T \mathbf{S} - \|-\mathbf{L}\mathbf{D}^\#\| \mathbf{S}^T \mathbf{S} \\
&\geq (1 - c_3) \|\mathbf{S}\|^2
\end{aligned} \tag{45}$$

With the utilization of the inequality (45), we can conclude:

$$\begin{aligned}
\dot{V}_2 &= - \left( k_1 - \frac{k_2}{2k} \right) \mathbf{S}^T \mathbf{S} - kk_2 \mathbf{v}^T \mathbf{v} - \frac{1}{2} \varepsilon_1 \tilde{c}_1^2 - \frac{1}{2} \varepsilon_2 \tilde{c}_2^2 \\
&\quad - \frac{1}{2} \varepsilon_3 \tilde{c}_3^2 + \frac{1}{2} \varepsilon_1 c_1^2 + \frac{1}{2} \varepsilon_2 c_2^2 + \frac{1}{2} \varepsilon_3 c_3^2 \\
&\leq -vV_1 + \sigma_1
\end{aligned} \tag{46}$$

with  $v = \min \{ (k_1 - \frac{k_2}{2k})/\bar{J}, k_2/(k\bar{J}), p_1\varepsilon_1, p_2\varepsilon_2, p_3\varepsilon_3 \}$  and  $\sigma_1 = \frac{1}{2}\varepsilon_1 c_1^2 + \frac{1}{2}\varepsilon_2 c_2^2 + \frac{1}{2}\varepsilon_3 c_3^2$

b).  $\hat{u}\|\mathbf{S}\| < \varepsilon$

$$\begin{aligned} \dot{V}_2 &\leq - \left( k_1 - \frac{k_2}{2k} \right) \mathbf{S}^T \mathbf{S} - kk_2 \mathbf{v}^T \mathbf{v} - \frac{1}{2}\varepsilon_1 \tilde{c}_1^2 - \frac{1}{2}\varepsilon_2 \tilde{c}_2^2 \\ &\quad - \frac{1}{2}\varepsilon_3 \tilde{c}_3^2 + \frac{1}{2}\varepsilon_1 c_1^2 + \frac{1}{2}\varepsilon_2 c_2^2 + \frac{1}{2}\varepsilon_3 c_3^2 \\ &\quad - \frac{\|\mathbf{S}\|^2 \hat{u}^2}{\varepsilon} + \|\mathbf{S}\| \hat{u} \\ &\leq - \left( k_1 - \frac{k_2}{2k} \right) \mathbf{S}^T \mathbf{S} - kk_2 \mathbf{v}^T \mathbf{v} - \frac{1}{2}\varepsilon_1 \tilde{c}_1^2 - \frac{1}{2}\varepsilon_2 \tilde{c}_2^2 \\ &\quad - \frac{1}{2}\varepsilon_3 \tilde{c}_3^2 - \left( \frac{\|\mathbf{S}\| \hat{u}}{\sqrt{\varepsilon}} - \frac{\sqrt{\varepsilon}}{2} \right)^2 \\ &\quad + \frac{1}{2}\varepsilon_1 c_1^2 + \frac{1}{2}\varepsilon_2 c_2^2 + \frac{1}{2}\varepsilon_3 c_3^2 + \frac{\varepsilon}{4} \\ &\leq -\nu V_2 + \sigma_2 \end{aligned} \tag{47}$$

where the inequality (45) is used and  $\sigma_2 = \frac{1}{2}\varepsilon_1 c_1^2 + \frac{1}{2}\varepsilon_2 c_2^2 + \frac{1}{2}\varepsilon_3 c_3^2 + \frac{1}{4}\varepsilon$ .

It can be concluded from (46) and (47) that the set  $\Omega = \{(\mathbf{S}, \mathbf{v}, \tilde{c}_1, \tilde{c}_2, \tilde{c}_3) \mid V_2 < \sigma_2/v\}$  is globally attractive. It is also noted that  $|S| \leq \sqrt{2V_2/\bar{J}} \leq \sqrt{2\sigma_2/v\bar{J}}$ ,  $|v| \leq \sqrt{2V_2/k^2\bar{J}} \leq \sqrt{2\sigma_2/vk^2\bar{J}}$  and  $|\tilde{c}_i| \leq \sqrt{2p_i V_2} \leq \sqrt{2p_i \sigma_2/v}$  ( $i = 1, 2, 3$ ). That is,  $\mathbf{S}, v$  are UUB. Since  $v$  is bounded, the prescribed performance requirement is guaranteed.

**Case II.**  $\|\mathbf{S}\| = 0$

When  $\|\mathbf{S}\| = 0$ , we can conclude that  $\boldsymbol{\omega}_e^o = -k\mathbf{v}$ . Then

$$V_1 = k^2 \mathbf{v}^T \mathbf{J} \mathbf{v} = \boldsymbol{\omega}_e^o T \mathbf{J} \boldsymbol{\omega}_e^o \tag{48}$$

Taking the time derivation of (48) and substituting (27), we get

$$\dot{V}_1 = 2\boldsymbol{\omega}_e^o T (\mathbf{f} + \mathbf{U}_c - \mathbf{L}\mathbf{D}^\# \mathbf{U}_c) \tag{49}$$

It is also noted that

$$\mathbf{U}_c = -k_2 \mathbf{v} = -\frac{k_2}{k} \boldsymbol{\omega}_e^o \tag{50}$$

Substituting (50) into (49), we obtain

$$\begin{aligned}\dot{V}_1 &= -\frac{2k}{k_2} \boldsymbol{\omega}_e^{oT} (I_3 - \mathbf{L}\mathbf{D}^\#) \boldsymbol{\omega}_e^o + \boldsymbol{\omega}_e^{oT} \mathbf{f} \\ &\leq -\frac{2(1-c_3)k}{k_2} \boldsymbol{\omega}_e^{oT} \boldsymbol{\omega}_e^o + \bar{\omega}_e^o \bar{f}\end{aligned}\tag{51}$$

Same as in Case I, we can get a globally attractive set  $\Omega^o = \left\{ \boldsymbol{\omega}_e^o \text{ or } \mathbf{v} \mid V_1 \leq \frac{\bar{\omega}_e \bar{f} k_2}{2(1-c_3)k} \right\}$ . Besides,  $|\boldsymbol{\omega}_e^o| \leq \sqrt{V_1/\bar{J}} \leq \sqrt{\bar{\omega}_e \bar{f} k_2/2(1-c_3)k\bar{J}}$  and  $|\mathbf{v}| \leq \sqrt{V_1/k^2\bar{J}} \leq \sqrt{\bar{\omega}_e \bar{f} k_2/2(1-c_3)k^3\bar{J}}$  are also UUB.

In both Case I and Case II,  $v$  is controlled to be ultimately uniformly bounded, and thus the prescribed performance guaranteed attitude tracking is achieved. This completes the proof.  $\square$

In practice, the feed-forward compensation part  $\mathbf{U}_{c_1}^{com}$  can be relaxed to avoid the discontinuous of  $\mathbf{U}_c$ . Then the controller becomes:

$$\mathbf{U}_c = -k_1 \mathbf{S} - k_2 \mathbf{v} + \mathbf{U}_{c_2} \tag{52}$$

with  $\mathbf{U}_{c_2}$  expressed by equation (32) to (34). This controller is adopted in the simulation and the simulation results show the stability under this controller (52).

*Remark 1:* Even though we assumed quite a lot of the upper bound of the signal such as  $\bar{J}$ ,  $\bar{\omega}$ ,  $\Delta_D$ ,  $\bar{l}$ , the majority of them are not used in the controller design process. Only the parameter  $c_3$  which estimates the worst case of the control signal degradation is synthesized in the controller design. This makes the controller design realizable when the assumed upper bounds are unknown.

#### 4. Numerical Simulation

In this section, numerical simulations are conducted for a rigid spacecraft. The inertia matrix is  $\mathbf{J} = [20 \ 1.2 \ 0.9; \ 1.2 \ 17 \ 1.4; \ 0.9 \ 1.4 \ 15] \text{kgm}^2$ . A cluster of four actuators are installed in a pyramid configuration, i.e.  $\mathbf{D} = \frac{1}{\sqrt{3}}[-1 \ -1 \ 1; \ 1 \ -1 \ -1; \ 1 \ 1 \ 1]$ . The misalignment  $\Delta\mathbf{D}$  is assumed to be 0.2% $\mathbf{D}$ . The

initial attitude of the spacecraft is chosen as  $\mathbf{Q}(0) = [0.9211, -0.23, 0.19, 0.25]^T$  and  $\boldsymbol{\omega}(0) = [0, 0, 0]^T$  rad/s. The initial attitude of the virtual spacecraft is chosen as  $\mathbf{Q}_d(0) = [1, 0, 0, 0]^T$ . The angular velocity is set to be  $\boldsymbol{\omega}_d = 0.01[\cos(t/40), \sin(t/60), -\cos(t/5)]^T$  rad/s. The unit quaternion error is calculated via equation (3) and  $\boldsymbol{\omega}_e, \boldsymbol{\omega}_e^o$  are obtained via  $\boldsymbol{\omega}_e = \boldsymbol{\omega} - \mathbf{R}(\mathbf{Q}_e)\boldsymbol{\omega}_d$  or  $\boldsymbol{\omega}_e^o = \boldsymbol{\omega} + \mathbf{W}(t, \boldsymbol{\omega}) - \mathbf{R}(\mathbf{Q}_e)\boldsymbol{\omega}_d$  without or with gyro fault respectively.

Consider the external disturbances, which are assumed to be as in [27]:

$$d = 10^{-3} \times \begin{bmatrix} 3 \cos(10\omega_t t) + 3 \cos(10\omega_t t) - 10 \\ -1.5 \sin(2\omega_t t) + 3 \cos(5\omega_t t) + 15 \\ 3 \sin(10\omega_t t) - 8 \sin(4\omega_t t) + 10 \end{bmatrix} \text{Nm} \quad (53)$$

with  $\omega_t = 0.01$ .

The actuators are assumed to suffer from partial loss effectiveness or complete failure. The detailed fault scenarios are as in [20]:

$$\begin{cases} e_1(t) = 0.5 + 0.09 \sin(0.05t) + 0.005 \text{rand}(\cdot) \\ e_2(t) = 0.6 + 0.1 \cos(0.08t) + 0.008 \text{rand}(\cdot) \\ e_3(t) = 0.4 + 0.08 \sin(0.06t) + 0.005 \text{rand}(\cdot) \\ e_4(t) = 0 \end{cases} \quad (54)$$

The estimated effectiveness matrix is assumed as  $\widehat{\mathbf{E}}(t) = \text{diag}([0.5, 0.6, 0.4, 0])$ .

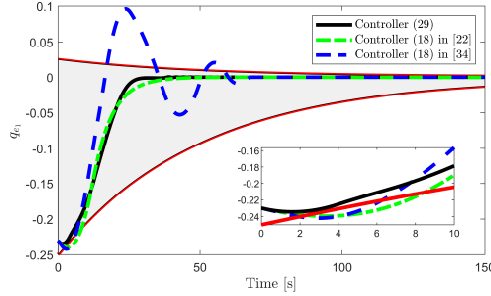
The performance indexes in (11) are listed in the following table 1:

Table 1: Performance index				
i	$\rho_i(0)$	$\rho_i(\infty)$	$\mu_i$	$\delta_i$
1	0.25	$1.4 \times 10^{-4}$	0.02	0.1
2	0.2	$1.4 \times 10^{-4}$	0.02	0.1
3	0.3	$1.4 \times 10^{-4}$	0.02	0.1

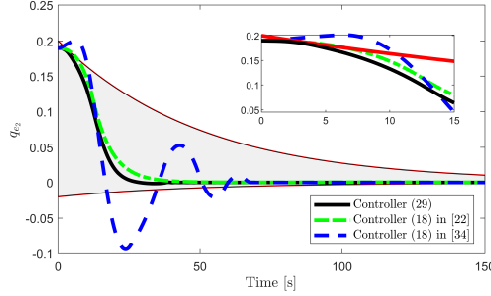
The remaining parameters are chosen as  $c_1(0) = 0.02, c_2(0) = 1, c_3(0) = 0.25, k = 0.02, k_1 = 2, k_2 = 5, p_1 = p_2 = p_3 = 1, \varepsilon = 0.001$ , and  $\varepsilon_1 = \varepsilon_2 = \varepsilon_3 = 0.1$ . The maximum control torque is set as 0.2 Nm.

*Case I:* Simulation results without gyro fault

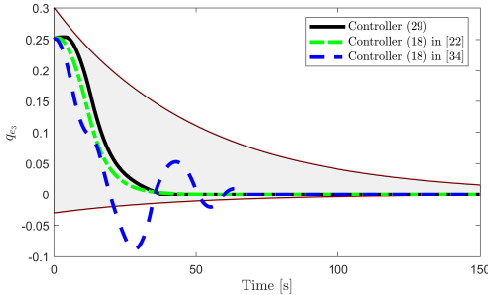
In this fault, we assume that the angular velocity can be measured accurately, i.e.  $\omega^o = \omega$ . Thus all the feedback signals such as  $\omega_e$  will be accurate. To verify the effectiveness of the proposed method, same numerical simulations are



(a)  $q_{e_1}$  and prescribed constraint



(b)  $q_{e_2}$  and prescribed constraint



(c)  $q_{e_3}$  and prescribed constraint

Figure 3: Trajectory of quaternion error without gyro fault

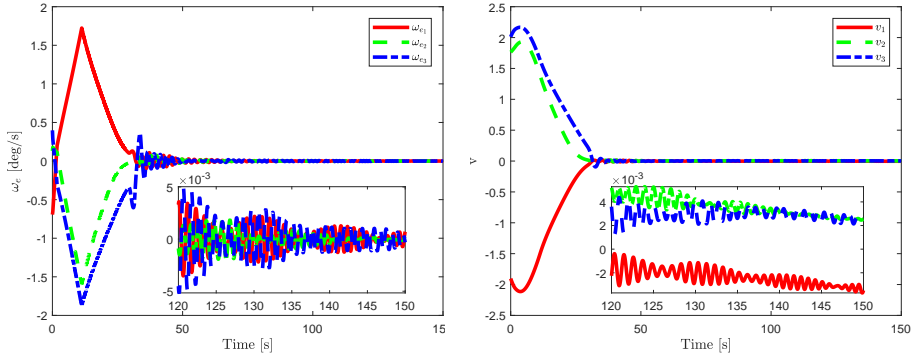


Figure 4:  $\omega_e$  without gyro fault

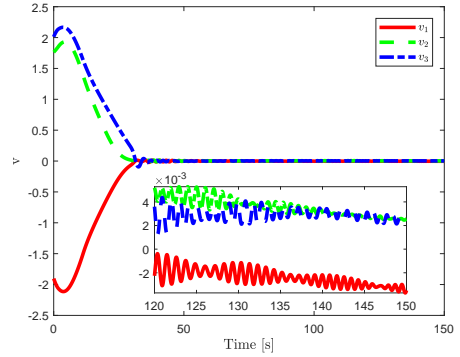


Figure 5:  $v$  without gyro fault

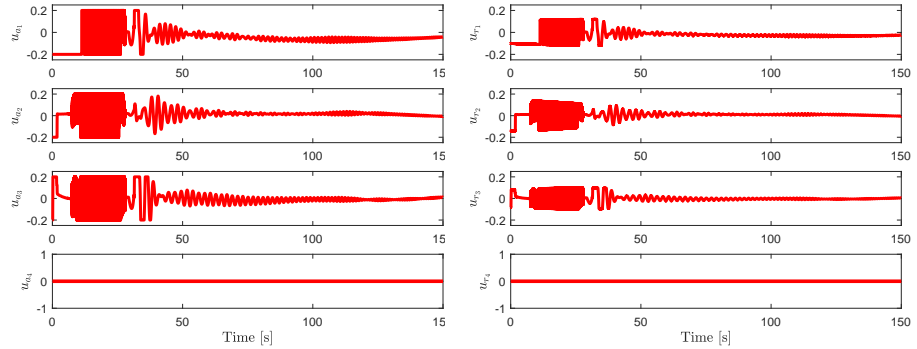


Figure 6:  $U_a$  without gyro fault

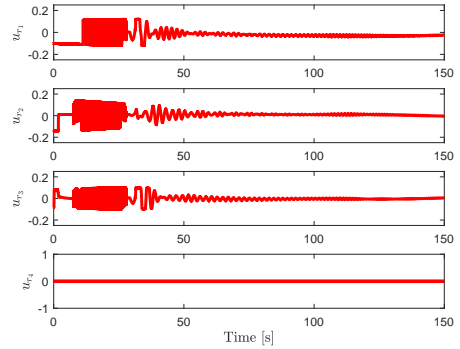


Figure 7:  $U_r$  without gyro fault

conducted based on the controller proposed in [20] and [33]. The same control gains are chosen according to [20] and [33] for comparison. Simulation results are shown in Fig. 3 to Fig. 8.

Fig. 3 illustrates the trajectory of the unit quaternion error without gyro fault and it is observed that attitude tracking can be achieved within 50 s. The components of the vector part of  $Q_e$  are shown in Fig. 3(a) to 3(c). It can be seen that the trajectories of the unit quaternion are controlled into the prescribed tube described by (15). Thus the prescribed performance, i.e. attitude tracking

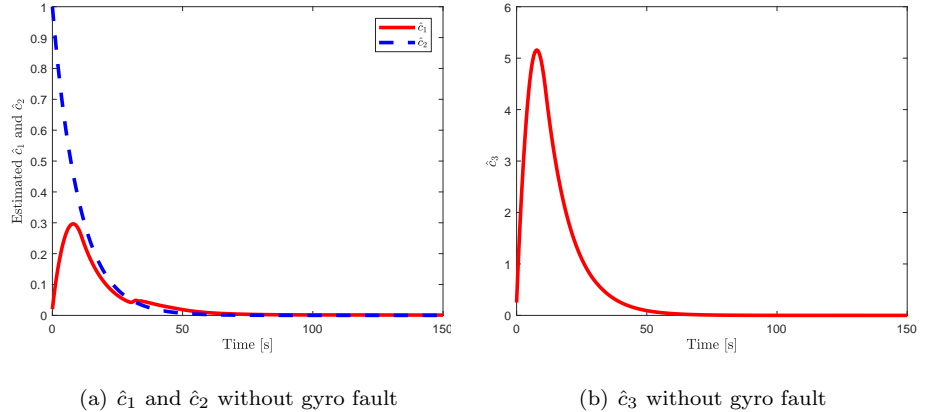


Figure 8: Estimated parameters without gyro fault

error converging to a small residual set, the converge rate being faster than the predefined value and the overshoot and undershoot being constrained, is guaranteed. However, the trajectories of  $q_{e1}$  and  $q_{e2}$  under the controller (18) of [20] or the controller (18) of [33] exceed the prescribed performance boundaries. Fig. 4 presents the time history of the angular velocity error  $\omega_e$  ( $\omega_e^o = \omega_e$  in this case).  $\omega_e$  converges to a small region and the maximum angular velocity error is smaller than 2 deg/s. Fig. 5 shows the convergence of the transformed state  $v$ , whose boundedness guarantees the prescribed performance. According to property 1,  $v$  going to zero implies  $q_{ev}$  converges to zero. Fig. 6 and Fig. 7 show the allocated control torque and actual output control torque correspondingly. Fig. 6 tells that the allocated control torque to the fourth actuator which totally fails is zero. This verifies the effectiveness of the CA method in (20), which minimizes the use of the faulty actuator. Fig. 7 demonstrates the actual output. The difference to Fig. 6 illustrates the actuator effectiveness given by (54). The estimated parameters are shown in Fig. 8.  $\hat{c}_1$ ,  $\hat{c}_2$  in Fig. 8(a) and  $\hat{c}_3$  in Fig. 8(b) are bounded. All of these estimated parameters converge to zero. In addition, all of these estimated parameters are greater than zero, which verifies the Property 2.

*Case II:* Simulation results with gyro fault

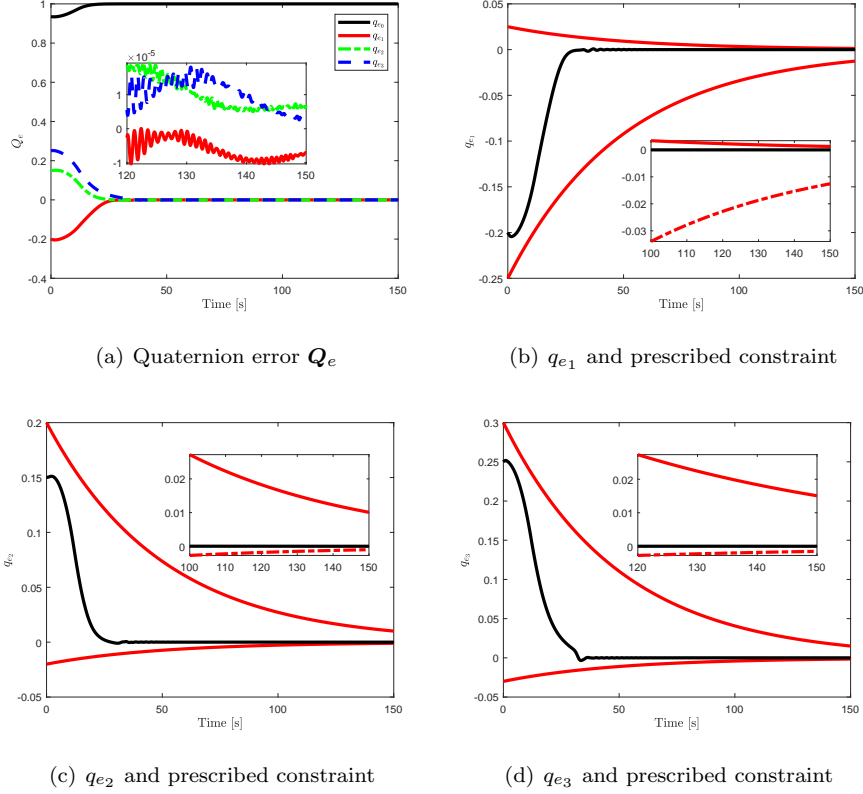


Figure 9: Trajectory of quaternion error without gyro fault

The sensor fault is considered in the scenario. The output of the measured angular velocity are assumed as:

$$\begin{cases} \omega_1^o(t) = (1 + 0.2 \sin(\frac{\pi}{15}t) + 0.1 \text{rand}(\cdot)) \omega_1(t) \\ \omega_2^o(t) = (1 + 0.2 \sin(\frac{\pi}{15}t + \frac{\pi}{3}) + 0.1 \text{rand}(\cdot)) \omega_2(t) \\ \omega_3^o(t) = (1 + 0.2 \sin(\frac{\pi}{15}t + \frac{2\pi}{3}) + 0.1 \text{rand}(\cdot)) \omega_3(t) \end{cases} \quad (55)$$

It can be seen that the measurement of the angular velocity is corrupted with a periodic and random error, and the maximum magnitude of the measurement error is 30 percents of the actual value. The initial attitude is chosen to be  $\mathbf{Q}(0) = [0.9354, -0.2, 0.15, 0.25]^T$ .

These measured values marked with a superscript ‘o’ are only used in controller design in simulation, and the actual value are used as the input of the

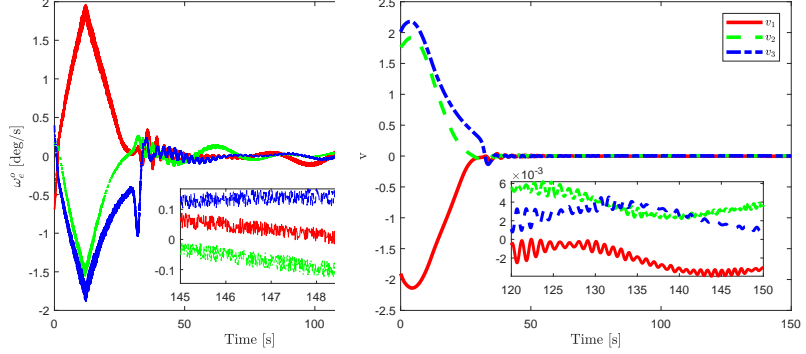


Figure 10:  $\omega_e$  with gyro fault

Figure 11:  $v$  with gyro fault

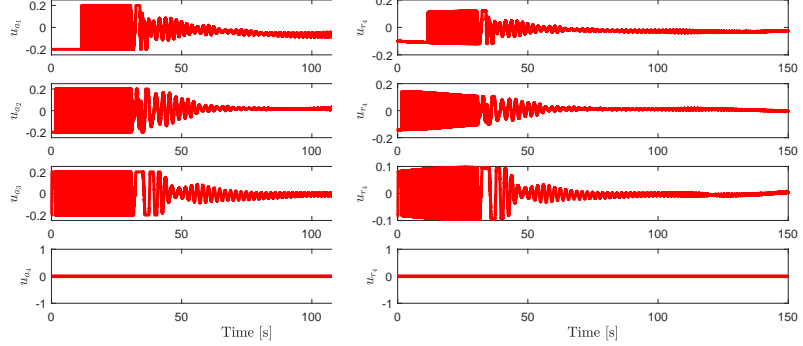


Figure 12:  $U_a$  with gyro fault

Figure 13:  $U_r$  with gyro fault

kinematics model. The simulation results are shown as in Fig. 9 and 14.

Fig. 9 shows that prescribed performance guaranteed attitude tracking is achieved. It gives that the tracking error converges to a small set within 50s. Similar to Fig. 3, the components of the vector part of the quaternion error converge to small values which are smaller than the predefined steady state error, and the rate of convergence is larger than the required speed as shown in Fig. 9(b) to Fig. 9(d). The control results under controllers in [20] and [33] are also similar to the results shown in Fig. 3 where the prescribed performance is

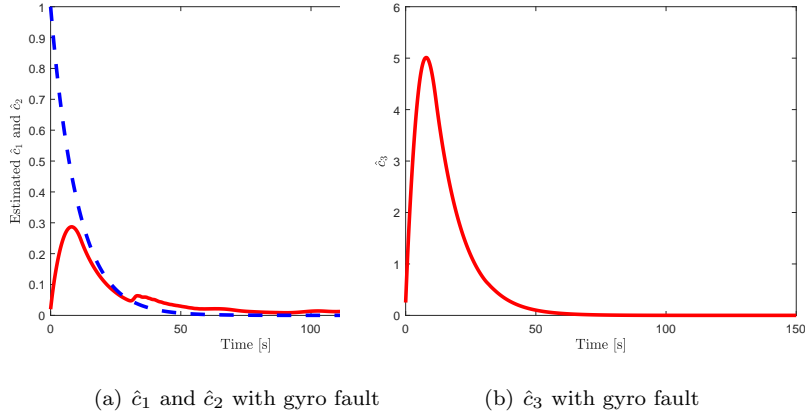


Figure 14: Estimated parameters with gyro fault

not guaranteed. Fig. 10 demonstrates the time history of the measured angular velocity error. It is clear that the demonstrated  $\omega_e^o$  does not converge to zero as in Fig. 10. The compromised angular velocity as in (55) is used to calculate  $\omega_e^o$ , which is further employed to compute command control torque. Fig. 11 shows the trajectory of the transformed state. The boundedness of transformed state in Fig. 11 guarantees the pre-designed performance requirement, and the convergence of  $v$  implies the convergence of  $q_{ev}$ . Similar to Fig. 6 and Fig. 7, Fig. 12 and Fig. 13 present the allocated control torque and the actual control torque under the fault scenarios in (54). All the estimated parameters  $\hat{c}_1$ ,  $\hat{c}_2$  and  $\hat{c}_3$  are shown in Fig. 14.

## 5. Conclusion

This paper investigates the attitude tracking problem of the rigid spacecraft suffering from actuators fault, misalignment and external disturbances simultaneously. In the process of the tracking, the tracking error is required to converge to a small residual set and the converge rate is required to be larger than a predesigned value with requirements in overshoot and undershoot. These prescribed performance requirements are transformed into a new state, whose boundedness is sufficient and necessary to guarantee the performance require-

ment. Using this transformed state, a robust adaptive sliding mode controller is developed. In addition, a  $L_2$ -CA method is employed to minimize the use of faulty actuator. The overall proposed fault-tolerant control system achieves attitude tracking with prescribed performance. Numerical simulation results verify the effectiveness of the proposed controller.

### Supporting information

To verify the assumption of  $c_3 < 1$ , the true value of  $\|\mathbf{LD}^\#\|$  during the maneuver is demonstrated as follows:

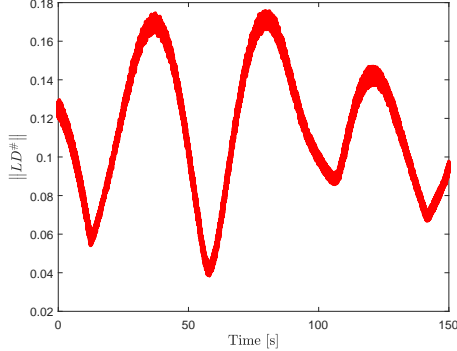


Figure 15: Value of  $\|\mathbf{LD}^\#\|$  during the simulation without gyro fault

It is clearly observed that the maximum of  $\|\mathbf{LD}^\#\|$  is less than 0.2. In the simulation, we choose  $c_3 = 0.25$ . Therefore, the inequality  $\|\mathbf{LD}^\#\| < c_3 < 1$  holds throughout the simulation .

- [1] JT-Y Wen and Kenneth Kreutz-Delgado. The attitude control problem. *IEEE Transactions on Automatic control*, 36(10):1148–1162, 1991.
- [2] A.H. Tahoun. Time-varying multiplicative/additive faults compensation in both actuators and sensors simultaneously for nonlinear systems via robust sliding mode control scheme. *Journal of the Franklin Institute*, 356(1):103 – 128, 2019.

- [3] Baolin Wu, Danwei Wang, and Eng Kee Poh. Decentralized sliding-mode control for attitude synchronization in spacecraft formation. *International Journal of Robust and Nonlinear Control*, 23(11):1183–1197, 2013.
- [4] An-Min Zou, Krishna Dev Kumar, and Anton HJ Ruiter. Robust attitude tracking control of spacecraft under control input magnitude and rate saturations. *International Journal of Robust and Nonlinear Control*, 26(4):799–815, 2016.
- [5] Yao Zou. Singularity-free adaptive fault-tolerant trajectory tracking controller for vtol uavs. *International Journal of Systems Science*, 48(10):2223–2234, 2017.
- [6] Taeyoung Lee. Exponential stability of an attitude tracking control system on so (3) for large-angle rotational maneuvers. *Systems & Control Letters*, 61(1):231–237, 2012.
- [7] Bing Xiao, Qinglei Hu, William Singhose, and Xing Huo. Reaction wheel fault compensation and disturbance rejection for spacecraft attitude tracking. *Journal of Guidance, Control, and Dynamics*, 36(6):1565–1575, 2013.
- [8] Bing Xiao, Qinglei Hu, Danwei Wang, and Eng Kee Poh. Attitude tracking control of rigid spacecraft with actuator misalignment and fault. *IEEE Transactions on Control Systems Technology*, 21(6):2360–2366, 2013.
- [9] YD Song and Wenchuan Cai. Quaternion observer-based model-independent attitude tracking control of spacecraft. *Journal of guidance, control, and dynamics*, 32(5):1476–1482, 2009.
- [10] Travis H Mercker and Maruthi R Akella. Rigid-body attitude tracking with vector measurements and unknown gyro bias. *Journal of guidance, control, and dynamics*, 34(5):1474–1484, 2011.
- [11] Miao Yu and Chaoyong Li. Robust adaptive iterative learning control for discrete-time nonlinear systems with time-iteration-varying param-

- ters. *IEEE Transactions on Systems, Man, and Cybernetics: Systems*, 47(7):1737–1745, 2017.
- [12] Shen Yin, Bing Xiao, Steven X Ding, and Donghua Zhou. A review on recent development of spacecraft attitude fault tolerant control system. *IEEE Transactions on Industrial Electronics*, 63(5):3311–3320, 2016.
- [13] Jianqing Li, Sai Chen, Chaoyong Li, Changsheng Gao, and Wuxing Jing. Adaptive control of underactuated flight vehicles with moving mass. *Aerospace Science and Technology*, 85:75–84, 2019.
- [14] Jin Jiang and Xiang Yu. Fault-tolerant control systems: A comparative study between active and passive approaches. *Annual Reviews in control*, 36(1):60–72, 2012.
- [15] F Landis Markley, Reid G Reynolds, Frank X Liu, and Kenneth L Lebsack. Maximum torque and momentum envelopes for reaction wheel arrays. *Journal of Guidance, Control, and Dynamics*, 33(5):1606–1614, 2010.
- [16] Dov Verbin, Vaios J Lappas, and Joseph Z Ben-Asher. Time-efficient angular steering laws for rigid satellite. *Journal of Guidance, Control, and Dynamics*, 34(3):878–892, 2011.
- [17] Xibin Cao, Chengfei Yue, Ming Liu, and Baolin Wu. Time efficient spacecraft maneuver using constrained torque distribution. *Acta Astronautica*, 123:320–329, 2016.
- [18] Ola Härkegård and S Torkel Glad. Resolving actuator redundancy — optimal control vs. control allocation. *Automatica*, 41(1):137–144, 2005.
- [19] Halim Alwi and Christopher Edwards. Fault tolerant control using sliding modes with on-line control allocation. *Automatica*, 44(7):1859–1866, 2008.
- [20] Qiang Shen, Danwei Wang, Senqiang Zhu, and Eng Kee Poh. Inertia-free fault-tolerant spacecraft attitude tracking using control allocation. *Automatica*, 62:114–121, 2015.

- [21] Xu Jin, Wassim M Haddad, and Tansel Yucelen. An adaptive control architecture for mitigating sensor and actuator attacks in cyber-physical systems. *IEEE Transactions on Automatic Control*, 62(11):6058–6064, 2017.
- [22] Abdelaziz Benallegue, Yacine Chitour, and Abdelhamid Tayebi. Adaptive attitude tracking control of rigid body systems with unknown inertia and gyro-bias. *IEEE Transactions on Automatic Control*, 2018.
- [23] Junmin Peng, Chaoyong Li, and Xudong Ye. Cooperative control of high-order nonlinear systems with unknown control directions. *Systems & Control Letters*, 113:101–108, 2018.
- [24] Charalampos P Bechlioulis and George A Rovithakis. Adaptive control with guaranteed transient and steady state tracking error bounds for strict feedback systems. *Automatica*, 45(2):532–538, 2009.
- [25] Charalampos P Bechlioulis and George A Rovithakis. Prescribed performance adaptive control for multi-input multi-output affine in the control nonlinear systems. *IEEE Transactions on Automatic Control*, 55(5):1220–1226, 2010.
- [26] Yongduan Song, Yujuan Wang, and Changyun Wen. Adaptive fault-tolerant pi tracking control with guaranteed transient and steady-state performance. *IEEE Transactions on automatic control*, 62(1):481–487, 2017.
- [27] Qinglei Hu, Xiaodong Shao, and Lei Guo. Adaptive fault-tolerant attitude tracking control of spacecraft with prescribed performance. *IEEE/ASME Transactions on Mechatronics*, 23(1):331–341, 2018.
- [28] Jianjun Luo, Caisheng Wei, Honghua Dai, Zeyang Yin, Xing Wei, and Jianping Yuan. Robust inertia-free attitude takeover control of postcapture combined spacecraft with guaranteed prescribed performance. *ISA transactions*, 74:28–44, 2018.

- [29] Jianjun Luo, Zeyang Yin, Caisheng Wei, and Jianping Yuan. Low-complexity prescribed performance control for spacecraft attitude stabilization and tracking. *Aerospace Science and Technology*, 74:173–183, 2018.
- [30] Abdelhamid Tayebi. Unit quaternion-based output feedback for the attitude tracking problem. *IEEE Transactions on Automatic Control*, 53(6):1516–1520, 2008.
- [31] Peter C Hughes. *Spacecraft attitude dynamics*. Courier Corporation, 2012.
- [32] Wei Wang and Changyun Wen. Adaptive actuator failure compensation control of uncertain nonlinear systems with guaranteed transient performance. *Automatica*, 46(12):2082–2091, 2010.
- [33] Wenchuan Cai, Xiaohong Liao, and David Y Song. Indirect robust adaptive fault-tolerant control for attitude tracking of spacecraft. *Journal of Guidance, Control, and Dynamics*, 31(5):1456–1463, 2008.